Journal of Manufacturing Processes 29 (2017) 133–148

Contents lists available at ScienceDirect

Journal of Manufacturing Processes

journal homepage: www.elsevier.com/locate/manpro

Technical Paper

Investigation into the effect of material properties and arrangement of each layer on the formability of bimetallic sheets

Roya Darabi [a,*], Hamed Deilami Azodi [a], Saeed Bagherzadeh [b]

[a] Department of Mechanical Engineering, Arak University of Technology, Arak, Iran
[b] School of Mechanical Engineering, College of Engineering, University of Tehran, Tehran, Iran

ARTICLE INFO

Article history:
Received 30 December 2016
Received in revised form 14 June 2017
Accepted 21 July 2017

Keywords:
Bimetallic sheets
Formability
Material properties
M-K model
Layers design

ABSTRACT

The application of bimetallic sheets composed of two dissimilar sheet metals with distinct properties has increasingly developed in recent years. Enhancement of bimetallic sheet's formability by designing of appropriate layers is an important challenge for industrialization of these sheets. The main objective of this paper is investigation on the influence of material properties of layers on the formability of bimetallic sheets analytically and experimentally. The analytical model was developed to predict forming limit diagram (FLD) based on M-K model using both the Hill's and Barlat-Lian yield functions. The experimental works was performed on Aluminum (AL3105)/Carbon steel (St14) sheets for verification of analytical model. Results showed that the formability of bimetallic sheet is enhanced by increasing of the strain hardening and strain rate sensitivity exponents of layers, although variation of the exponent coefficient of the layer with higher formability was more effective than layer with lower formability. In addition, the results demonstrated a significant nonlinear effect of variation in thickness of layers on the FLD_0 index. It is found that the influence of anisotropy coefficient of layers is negligible in comparison with other material parameters, but the arrangement of anisotropic steel layer with isotropic aluminum layer as well as the arrangement of layers in the aligned rolling direction (0°–0°) can slightly improve the formability of two-layer sheets.

1. Introduction

Recently, the application of laminated composite sheet metals and specially two-layer metallic sheets has been greatly increased due to achieving desirable mechanical, physical and chemical properties such as high strength low weight structures, vibration damping, corrosion resistance, appropriate thermal and electrical conductivity in the variant industries. Aluminum-steel (AL-St) sheet is one of the most common clad sheets, in which the cladding can be carried out by several methods such as clad rolling [1], adhesive bonding [2], explosive forming [3] and etc. These bimetallic sheets consist of two distinct metals as a high strength (St) layer bonded to a lightweight low formable (AL) layer. Therefore, their forming behavior is different that of each layer and it is worth to study the effect of material properties of each layer on the formability of two-layer sheet in order to optimum design of bimetallic sheets.

Forming limit diagram (FLD) is commonly used to evaluate the formability of sheet metals in metal forming processes. The FLD is a plot of the major strain versus the minor strain which is obtained at the onset of localized necking condition. This curve defines the maximum permissible major strain with respect to the minor strain above which failure may be occurred in the deformed sheet. The concept of FLD was introduced by Keeler [4] and Goodwin [5] for the first time in 1968. Besides of many researchers reported on the mono-sheets, the formability of two-layer sheets has been the subject of some researchers. Semiatin and Piehler[6,7] investigated the formability of stainless steel-clad aluminum and aluminum-clad stainless steel sheets based on defuse and localized necking. They resulted that the final localization and fracture are affected by arrangement of layers. Mori and Kurimoto [8] studied the formability of stainless steel-aluminum clad sheet experimentally. They utilized deep drawing process with a cylindrical punch and stretch forming test with a hemispherical punch to evaluate the formability of sheet. They concluded that a higher formability can be achieved when the aluminum is set on the outer side of the cup in stretching and deep drawing tests. Yoshida and Hino [9] determined the forming limits of sheet metal laminates under biaxial stress conditions. They developed a criterion for the left hand side

* Corresponding author. Mechanical Eng. Dep Arak University of Technology, PO. Box: 38135-1177, Arak, Iran.
E-mail address: Royadrb8989@gmail.com (R. Darabi).

http://dx.doi.org/10.1016/j.jmapro.2017.07.022
1526-6125/

Nomenclature

C	Strength coefficient
d_0	Grain size
$\boldsymbol{h}$	Coefficient of heterogeneity
k	Grain size coefficient
M	Hill's index
A	Barlat-Lian yield exponent
m	Strain rate sensitivity exponent
n	Strain hardening exponent
R_G	Initial surface roughness
r_0, r_{90}	Anisotropy coefficients at 0° *and* 90° from rolling direction
r	Normal anisotropy coefficient
α	Ratio of principle stress components
β	Ratio of effective strain increment to strain increment in direction1
ε_i	Principal strain component
$\bar{\varepsilon}$	Effective strain
ρ	Ratio of minor strain to major strain
σ_i	Principal stress components
σ_{ij}	Stress components
$\bar{\sigma}$	Effective stress
φ	Ratio of principal stress to effective stress
t	Sheet thickness
f	Yield function
$d\lambda$	Proportionality factor
S	Thickness ratio

of the FLD curve based on the Hill's localized necking theory. In addition, punch-stretching tests were done on two and three-ply stainless steel-clad aluminum sheets. Kim et al. [10] studied the formability of roll-bonded AA5182/polypropylene/AA5182 sandwich sheets. They used the M-K theory associated with Hill's yield function to predict FLD of sandwich sheet. They found out that higher thickness of sandwich sheet is main reason for improving of formability. Jalali et al. [11,12] investigated the formability of AL1100-St12 two-layer sheet analytically and experimentally. They predicted the FLD of two layer sheet lies between those of elements which compose it. They also studied the influence of mechanical properties of layers on the formability of bimetallic sheet. Bagherzadeh et al. [13,14] studied hydro-mechanical deep drawing of two-layer steel-aluminum sheets based on Barlat-Lian's anisotropy criterion analytically and experimentally. They demonstrated that the mechanical properties, thickness and arrangement of layers can influence limiting drawing ratio of bimetallic sheet. Liu et al. [15] performed numerical studies based on Gurson-Tvergaard-Needleman (GTN) damage model on the formability of AA5052/polyethylene/AA5052 sandwich sheet. They concluded that the sandwich sheet has a better formability than AA5052 mono-sheet and the increase of polyethylene layer thickness improves the formability of sandwich sheet. Parsa et al. [16,17] investigated the formability of Al 3105/Polypropylene/Al 3105 sandwich sheets theoretically and experimentally. They observed a good agreement between the numerical model based on GTN method and experimental works. Dehghani and Salimi[18] investigated the formability of copper-stainless steel 304L clad sheets in deep drawing numerically and experimentally. The influences of material properties, drawing ratio and thickness distribution of separate layers on the failure of two-layer part were evaluated. Comparison between experimental results and simulations showed that the finite element method can predict the effect of properties of each layer on two-layer part fracture sufficiently. Karajibani et al. [19] investigated the forming limit curve (FLC) of aluminum (1100)/copper (C10100) two-layer sheets obtained by numerical simulation based on two criteria including acceleration of the equivalent plastic strain and major strain. They concluded that the developed model verified by experiments can predict FLC of two-layer sheet desirably. Hashemi and Karajibani [20] obtained the forming limit diagram of aluminum–copper two-layer sheets by computational approach based on the modified M-K theory and experimental tests on equivalent two-layer sheet. They showed that there is a good agreement between the proposed method and experimental results. The use of equivalent approach can predict FLD of two-layer sheet with defined properties of layer, but, this approach need to obtain properties of composite sheet in variation of properties of each layer. Besides above mentioned numerical and experimental attempts, it is worth to investigate the formability of laminated sheets to extend fundamental understanding of forming processes.

In this paper, an analytical investigation was performed on the formability of two-layer sheets based on M-K model using Barlat-Lian and Hill's non-quadratic yield functions. A comprehensive parameter study was conducted to find out the influence of material properties of each layer. The analytical results were compared with those obtained from experiment on AL3105-St14 two-layer sheet to verify the developed model. The obtained results indicated the effectiveness of key properties of each layer on the final formability of bimetallic sheet.

2. Theoretical approach

2.1. The M-K model for two-layer sheets

The Marciniak-Kuczynski (M-K) [21] method is one of the most prominent technique to predict forming limit diagram (FLD). Based on the method, it is assumed that there is a narrow groove in the surface that is related to material inhomogeneity. Thus, there are two homogenous (area as "a") and inhomogeneous (area "b") regions as indicated in the Fig. 1. Developing M-K model can be done on the basis of the following assumptions:

(i) The groove is perpendicular to the maximum principal stress on material surface;
(ii) The in-plane stress condition is considered;
(iii) Thigh bonding condition is assumed between two sheet layers.

The general framework of M-K model for two-layer sheet metal deformation is described as follow. The coefficient of initial heterogeneity for mono-layer is expressed as:

$$h_0 = t_0^b / t_0^a \tag{1}$$

Where t_0^a and t_0^b are the initial thickness of homogenous and heterogeneous regions, respectively. The thickness of both regions has been changed during metal forming process which is defined as below:

$$t_{aorb} = t_0^{aorb} . \exp\left(\varepsilon_3^{aorb}\right) \tag{2}$$

Where ε_3^a and ε_3^b are the thickness strain. Also, the initial thickness of heterogeneous area (t_0^b) can be explained based on the homogenous region (t_0^a) as follow:

$$t_0^b = t_0^a - 2\left(R_G + k d_0 \bar{\varepsilon}^b\right) \tag{3}$$

Where R_G is the initial surface roughness, k is the coefficient of grain size, d_0 is the grain size and $\bar{\varepsilon}^b$ is the effective strain in the inhomo-

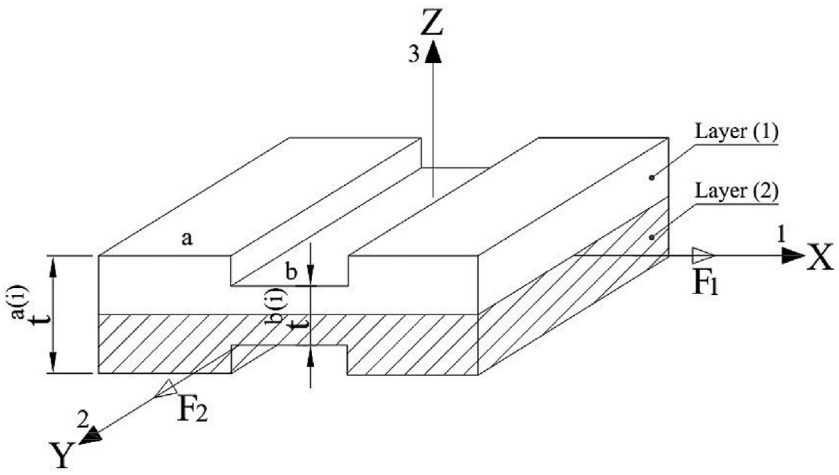

Fig. 1. The geometrical model considered in analytical model.

geneous region [22,23]. Hence, the coefficient of heterogeneity can be defined as:'

$$h = h_0 e^{\left(\varepsilon_3^b - \varepsilon_3^a\right)} \tag{4}$$

While the initial coefficient of heterogeneity for two-layer metallic sheet is specified as:

$$h_0 = \sum t_0^{b(i)} / \sum t_0^{a(i)} \tag{5}$$

Where $t_0^{a(i)}$ and $t_0^{b(i)}$are the initial thickness of homogeneous and heterogeneous regions fori^{th}layer. Considering the initial value of the coefficient of heterogeneity that is described by initial surface roughness and grain size, the coefficient of heterogeneity for each layer of bimetallic sheet during deformation can be determined by:

$$\boldsymbol{h} = \left(\left(\boldsymbol{t}_0^{\boldsymbol{a(i)}} - 2\left(\boldsymbol{R}_{\boldsymbol{G}}^{\boldsymbol{(i)}} + \boldsymbol{k}^{\boldsymbol{(i)}}\boldsymbol{d}_0^{\boldsymbol{(i)}}\bar{\boldsymbol{\varepsilon}}^{\boldsymbol{b(i)}}\right)\right).\boldsymbol{exp}\left(\boldsymbol{\varepsilon}_3^{\boldsymbol{b(i)}} - \boldsymbol{\varepsilon}_3^{\boldsymbol{a(i)}}\right)\right)/\boldsymbol{t}_0^{\boldsymbol{a(i)}} \tag{6}$$

According to the M-K model, the loading of sheet metal in the homogenous region progresses until the localize necking occurs in the heterogeneous region. In this condition, the strain increments on each sheet layers are grown until one of the following inequalities is established:

$$d\bar{\varepsilon}^{b(i)} / d\bar{\varepsilon}^{a(i)} \geq N\,(i = 1, 2) \tag{7}$$

Where, $d\bar{\varepsilon}^{b(i)}$ and $d\bar{\varepsilon}^{a(i)}$ are the equivalent strain increment of defected zone and safe zone in the layer (i) respectively. Also, N is a big enough number that indicates failure in the defected area. A common assumption is N = 10 as considered by previous references[11,20].Hence, the analytical approach is presented to predict the stress-strain states of each layer in the defected zone during loading process.

The compatibility requirement between the regions "a" and "b" yields to equality of strains at direction "2" of two regions for each layer in the loaded bimetallic sheet as [21]:

$$d\varepsilon_2^{b(i)} = d\varepsilon_2^{a(i)} \tag{8}$$

In addition, during loading of whole bimetallic sheet from end of sheet boundary in the direction "1", both safe (a) and defected (b) zones are loaded by a similar force (F_1). This equilibrium condition is expressed as:

$$\sum_{i=1}^{2} F_1^{a(i)} = \sum_{i=1}^{2} F_1^{b(i)} \tag{9}$$

In which $F_1^{a(i)}$ and $F_1^{b(i)}$are applied forces in the regions "a" and "b" for layer "i". With eliminating same width of sheet in different zones, the above equation can be rewritten based on the effective stress ($\bar{\sigma}^{a,b(i)}$) and thickness of sheet $\left(t^{a,b(i)}\right)$ in different regions as follows:

$$\sum_{i=1}^{2} \frac{\sigma_1^{a(i)}}{\bar{\sigma}^{a(i)}} \bar{\sigma}^{a(i)} t^{a(i)} = \sum_{i=1}^{2} \frac{\sigma_1^{b(i)}}{\bar{\sigma}^{b(i)}} \bar{\sigma}^{b(i)} t^{b(i)} \tag{10}$$

Where, the ratio of principal stress $\left(\sigma_1^{a,b(i)}\right)$ to effective stress $\left(\bar{\sigma}^{a,b(i)}\right)$ is defined as a variable $\varphi^{(i)} = \sigma_1^{a,b(i)} / \bar{\sigma}^{a,b(i)}$ under plane stress condition. Considering isotropic work hardening and strain rate hardening, the effective stress for each layer $\left(\bar{\sigma}^{(i)}\right)$ in the both regions can be predicted by Swift's equation [24] as:

$$\bar{\sigma}^{(i)} = C^{(i)}\left(\bar{\varepsilon}^{(i)}\right)^{n^{(i)}} \left(\dot{\bar{\varepsilon}}^{(i)}\right)^{m^{(i)}} \tag{11}$$

Where$C^{(i)}$,$n^{(i)}$,$m^{(i)}$ are the strength coefficient, strain hardening exponent and strain rate sensitivity exponent of the sheet metal material, respectively. Now, the yield function must be specified to calculate the $\bar{\varepsilon}^{(i)}$ for both regions of each layer. In this research, both Barlat-Lian and Hill's non-quadratic yield criteria have been utilized.

2.2. Anisotropic yield criteria

Barlat-Lian [25] yield function under plane stress condition in term of principal stress components (σ_1, σ_2) is expressed as:

$$|\sigma_1|^A + |u\sigma_2|^A + \frac{c}{2-c}|\sigma_1 - u\sigma_2|^A = \frac{2}{2-c}\bar{\sigma}^A \tag{12}$$

Where A is the exponent of yield function which defines the yield surface shape. This exponent is 8 for FCC and 6 for BCC materials [25]. The coefficients u and c can be determined as:

$$c = 2\sqrt{\frac{r_0}{1+r_0}\frac{r_{90}}{1+r_{90}}} \tag{13}$$

$$u = \sqrt{\frac{r_0}{1+r_0}\frac{1+r_{90}}{r_{90}}} \tag{14}$$

For planar isotropy($r_0 = r_{90} = r$), the coefficient ($u = 1$) and parameters c is as follows:

$$c = 2r/(1+r) \tag{15}$$

Where, the r_0 and r_{90} are the anisotropic coefficients in the direction 0° and 90° respect to the rolling direction of sheet metal. Also, the

parameter r is called normal anisotropy in the Hill's non-quadratic yield function. So, the effective strain of each layer $\bar{\varepsilon}^{(i)}$ can be determined by using Prandtle-Reuss flow rule as:

$$d\varepsilon_{ij} = d\lambda \frac{\partial f}{\partial \sigma_{ij}} \tag{16}$$

Where $d\lambda$ is the proportionality factor and f is the yield function. By using Barlat-Lian yield criteria associated by Prandtle-Russ law, the effective strain increment-effective stress ration is expressed as:

$$\begin{aligned} &\frac{d\varepsilon_1}{sign(\sigma_1)|\sigma_1|^{A-1} + sign(\sigma_1+\sigma_2)\frac{c}{2-c}|\sigma_1+\sigma_2|^{A-1}} \\ &= \frac{d\varepsilon_2}{sign(\sigma_2)|\sigma_2|^{A-1} - sign(\sigma_1-\sigma_2)\frac{c}{2-c}|\sigma_1-\sigma_2|^{A-1}} \\ &= \frac{-d\varepsilon_3}{sign(\sigma_1)|\sigma_1|^{A-1} + sign(\sigma_2)|\sigma_2|^{A-1}} = \frac{d\bar{\varepsilon}}{\frac{c}{2-c}\bar{\sigma}^{A-1}} \end{aligned} \tag{17}$$

Where, $d\varepsilon_1$, $d\varepsilon_2$,$d\varepsilon_3$are the plastic strain incremental components along the principal directions $(1, 2, 3)$ and$d\bar{\varepsilon}$ is effective strain increment.

Now, the stress-strain relationship of each layer of bimetallic sheet can be expressed in the both regions of sheet can be determined.

Similarly, the Hill's non-quadratic yield function [26] is expressed as:

$$\begin{aligned} &J|\sigma_2-\sigma_1|^M + G|\sigma_3-\sigma_1|^M + O|\sigma_1-\sigma_2|^M + P|2\sigma_1-\sigma_2-\sigma_3|^M \\ &+Q|2\sigma_2-\sigma_1-\sigma_3|^M + L|2\sigma_3-\sigma_1-\sigma_2|^M = \bar{\sigma}^M \end{aligned} \tag{18}$$

Where J, G, O, P, Q and L are defined after tensile tests according to the anisotropy parameters in the different directions and M is the exponent of yield criteria which defines the yield surface shape. This exponent is derived from experimental examinations refer to the approach by Dariani and Azodi [27], that are calibrated M_1(St14)=2.7 and M_2(AL3105)=2.3 in this study. Under the plane stress condition and planar isotropy, the yield function is written as follows:

$$|\sigma_1+\sigma_2|^M + (2r+1)|\sigma_1-\sigma_2|^M = 2(r+1)\bar{\sigma}^M \tag{19}$$

Again, by using Hill's yield function associated with Prandtle-Reuss law, the equivalent stress-strain relationship can be obtained as follows:

$$\begin{aligned} &\frac{d\varepsilon_1}{sign(\sigma_1+\sigma_2)|\sigma_1+\sigma_2|^{M-1} + sign(\sigma_1-\sigma_2)(1+2r)|\sigma_1-\sigma_2|^{M-1}} \\ &= \frac{d\varepsilon_2}{sign(\sigma_1+\sigma_2)|\sigma_1+\sigma_2|^{M-1} - sign(\sigma_1-\sigma_2)(1+2r)|\sigma_1-\sigma_2|^{M-1}} \\ &= \frac{-d\varepsilon_3}{2sign(\sigma_1+\sigma_2)|\sigma_1+\sigma_2|^{M-1}} = \frac{d\bar{\varepsilon}}{2(1+r)\bar{\sigma}^{M-1}} \end{aligned} \tag{20}$$

2.3. Prediction of forming limit diagram (FLD)

In the forming process, the loading condition is such that the strain path is proportional. So, the parameter $\rho = d\varepsilon_2/d\varepsilon_1$, which is defined as the ratio of the increments of principal strains will be constant. Based onincompressibility rule of plastic flow, the thickness strain is given as: $\boldsymbol{d\varepsilon_3 = d\varepsilon_2 + d\varepsilon_1}$. Accordingly, the ratio of principal stresses has been denoted as $\alpha = \sigma_2/\sigma_1$ can be determined using yield function Eqs. (17) or (20) and a given strain ratio ρ. Also, the ratio of principal stress (σ_1) to effective stress $(\bar{\sigma})$ is defined as a variable $\varphi = \sigma_1/\bar{\sigma}$ and the ratio $\beta = d\bar{\varepsilon}/d\varepsilon_1$ is specified as the ratio of effective strain $(d\bar{\varepsilon})$ to principal strain $(d\varepsilon_1)$ increments during forming limit diagram calculations.

The major-minor strain values to specify the boundary of FLD curve for two-layer sheet under deformation process is defined according to above mentioned analytical approach using instability Eq. (7). Accordingly, the initial values $\rho = -0.5$ and $d\varepsilon_1 = 0.005$ are assumed for safe region of layers while the strain values for defected region is undefined. The values of $\alpha^{b(i)}$ is defined for both layers. Then, the values of $\rho^{b(i)}$ and $\beta^{b(i)}$are determined with calculated $\alpha^{b(i)}$ for defected area of both layers. So, with considering compatibility equation (8) and determined values of $\beta^{b(i)}$, the effective strain of defected area for both layers is calculated.

Firstly, the set of parametric equations was developed in Maple software and then solving of nonlinear equations and plotting of the FLD curves were performed in MATLAB software. Fig. 2 shows a schematic flow chart of the presented algorithm.

Table 1
Material property of AL-3105 and St-14 sheets

Variables	Values	
Material	St14	AL3105
Thickness, t_0 (mm)	0.5	0.5
Young's modulus, E (MPa)	210000	70000
Poisson's ratio	0.3	0.33
Density, (Kg/m^3)	7850	2700
Strength coefficient, C (MPa)	548.44	302
Strain hardening exponent, n	0.229	0.103
Strain rate sensitivity exponent, m	0.01	0.001
Surface roughness, R_G (μm)	4	1.6
Anisotropy parameter, r	1.51	0.26
Grain size, d_0 (μm)	10	20

3. Experimental procedure

In order to verify the presented analytical model, a set of experimental works were carried out to examine the forming limit diagrams by out of plane stretching tests as proposed by Gosh and Hecker [28]. The experimental set-up is shown in Fig. 3a. The test specimens were machined of 0.5-mm-thickness sheet of Carbon steel (St-14) and 0.5-mm-thickness sheet of aluminum alloy (AL-3105). The geometry of die components for hemispherical stretch forming tests is illustrated in Fig. 3b. Material properties of used sheet metals are shown in Table 1.

The separate sheet layers were degreased with acetone and then were attached together by small layer of polyurethane adhesive. The geometry of the prepared specimens is shown in Fig. 4. As shown in this figure, four notched specimens (sample No. $1 \sim 4$) with various widths were used to examine left side of FLD curve and four rectangular specimens (sample No. $5 \sim 8$) were utilized to determine right side of FLD curve of two-layer sheet (Fig. 5a).

All tests were carried out by a 25-Ton hydraulic press with ram speed of 5 mm/min. Based on the circle grid analysis (CGA) method, several 5 mm diameter circular grids were printed on surface of the specimens for measuring of the strain components experimentally. For each specimen, the major and minor strains are measured from deformed grids in necking region. The steel side of two-layer AL/St samples was in contact with hemispherical punch. Fig. 5b shows the deformed notched samples after stretch forming process. As shown in this figure,

To evaluate "M" index of Hill yield function, a series of single layer 0.5-mm thickness specimen of St14 and AL3105 sheets were tested with same geometries as described in Figs. 4 and 5. The obtained FLD curves of each layer as well as combined two-layer sheet are shown in Fig. 6a. The indexes M_1 and M_2 are calibrated using the interpolated polynomial curves.

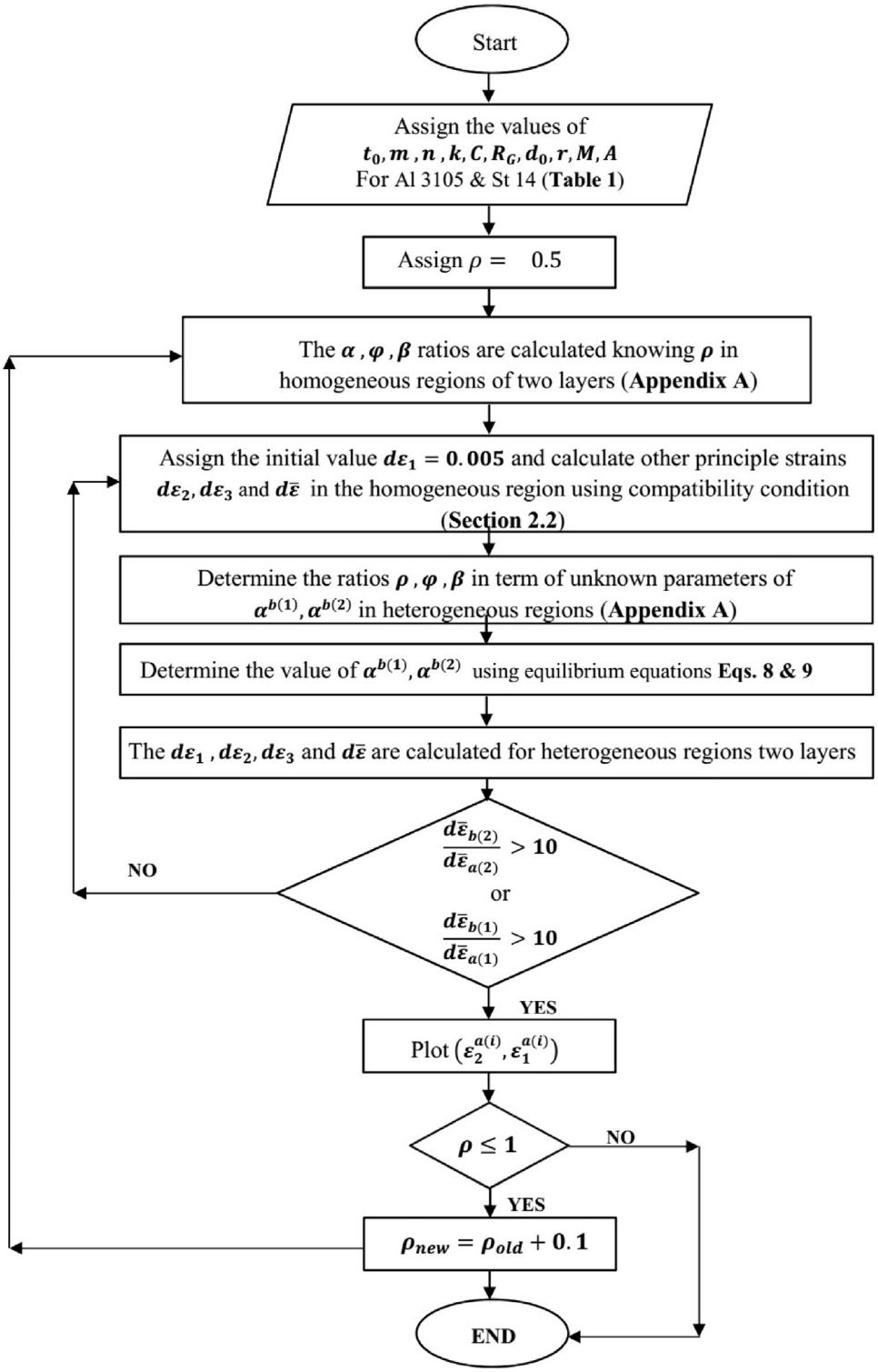

Fig. 2. Schematic procedure for calculation of FLD curve of two-layer sheets.

The deformed specimens of separate aluminum and steel sheets and two-layer sheet have been shown in the Fig. 6b. The measured curves show that the FLD of two-layer sheet is obtained between aluminum and steel single layers. As seen from experiment samples in the Fig. 6b, the steel sample was failed with higher straining of circles and higher dome height than aluminum sample with lower stretching and lower dome height. Also, the fractured sample of two-layer sheet demonstrates obviously that failure of aluminum layer is happened more quickly in respect of steel layer (Fig. 6c). It can be drawn as a reason for lowering of FLD of two-layer sheet than steel layer.

4. Results and discussion

The forming limit diagram of AL3105-St14 two-layer sheet is determined using analytical model based on M-K method with both Barlat-Lian and Hill's non-quadratic yield function. Also, the minor-major strains in rupture threshold have been measured

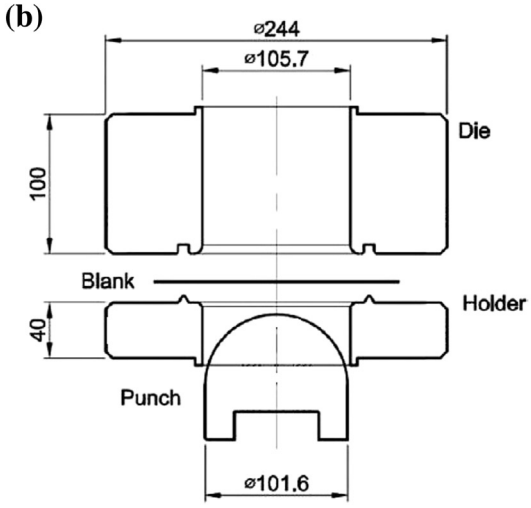

Fig. 3. (a) A view of experimental set-up, (b) geometry of hemispherical stretch forming die.

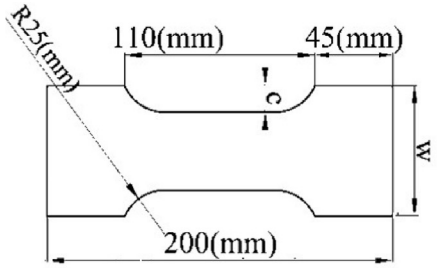

Sample No.	1	2	3	4	5	6	7	8
W(mm)	75	100	125	150	125	150	175	200
C(mm)	17.5	25	25	25	-	-	-	-

Fig. 4. The geometry of experimental test specimens.

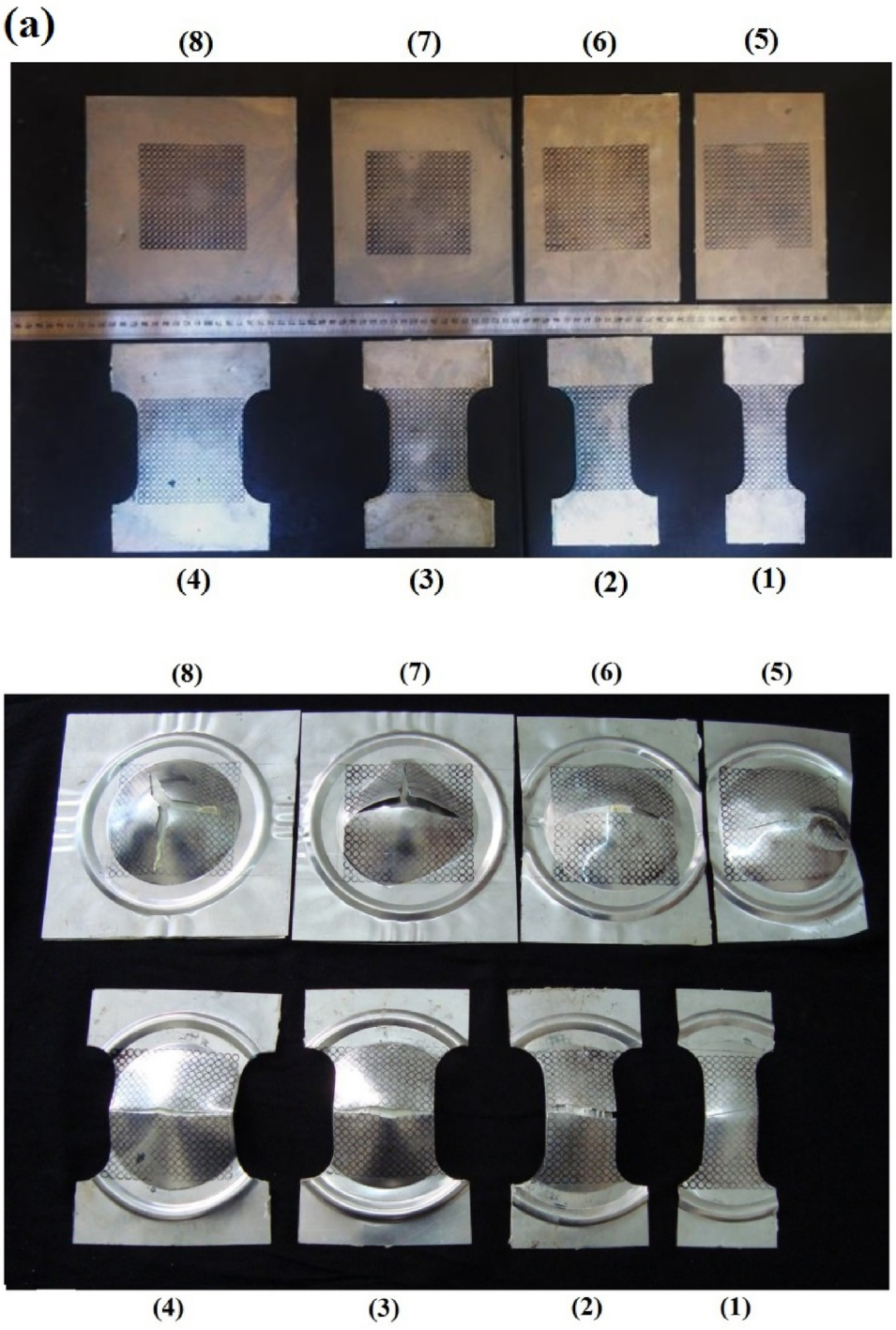

Fig. 5. (a) The prepared test samples, (b) The deformed samples after stretch forming.

experimentally. Fig. 7 shows a comparison between predicted FLD curves with both analytical approaches and experiments for the AL3105-St14 two-layer sheet that rupture may occur above these curves. As it can be seen from figure, the anisotropic criteria of the yield function has significant influence on the predicted FLD curve, however the obtained results of the lower point (FLD_0) based on the Hill's criteria and Barlat-Lian are the same. The results indicate that the FLD obtained using Barlat-Lian yield function has better compatibility with experimental observations on both tension-compression (left-side) and tension–tension (right-side) regions of FLD curve. Accordingly, in the previous study [29] on the effect of different yield functions on the forming limit diagram of Al-Li alloy, it was demonstrated that Barlat-Lian yield function as well as Hosford yield function was closer to the experimentally measured curve than Hill yield function. However, the prediction of all yield functions was near in the planar strain state (point FLD_0). In addition, an analytical approach conducted by [11] to predict FLD curve of steel, aluminum and Al/St sheets using Hill yield function confirms that Hill yield function cannot estimate left-side of FLD curve (tension-compression state) for AL and AL/St sheets. It can be concluded that both analytical models predict an upper bound of FLD curve for two-layer sheet properly but the predicted FLD

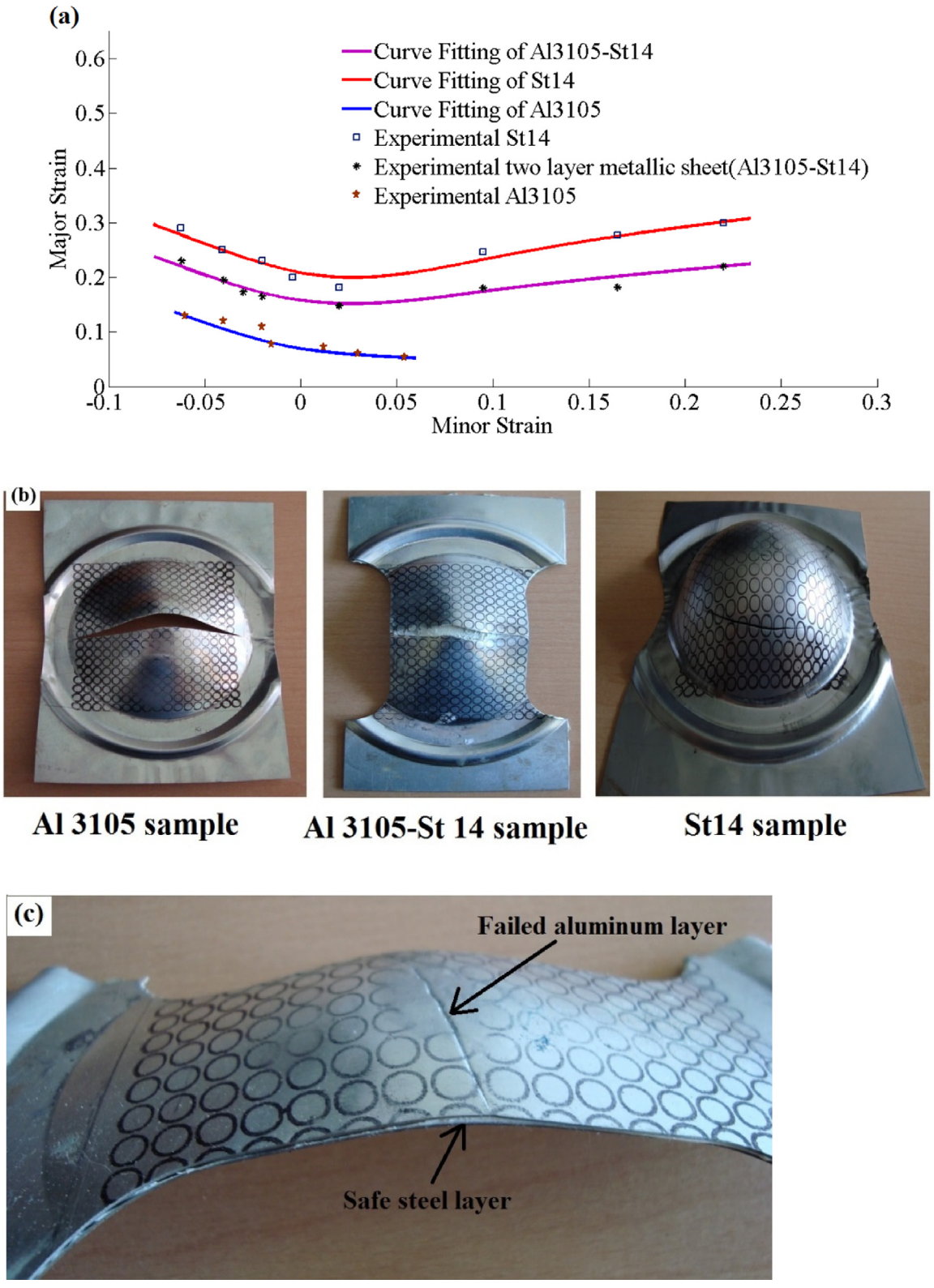

Fig. 6. (a) The measured FLD curves offal, St and AL-St sheets, (b) Fractured samples of separate aluminum and steel sheets versus aluminum-steel two-layer sheet; (c) Section view of fractured Al-St sample.

curve based on Barlat-Lian yield function is more accurate in both sides of curve with experimental observations. Hence, the results obtained from Barlat-Lian yield function was used for parameter studies.

4.1. Parametric study

4.1.1. Effect of strain hardening exponent of layers

Fig. 8(a, b) show the effect of strain hardening exponent (n_i) of layers on the FLD of two-layer sheet. In the Fig. 8a, the strain

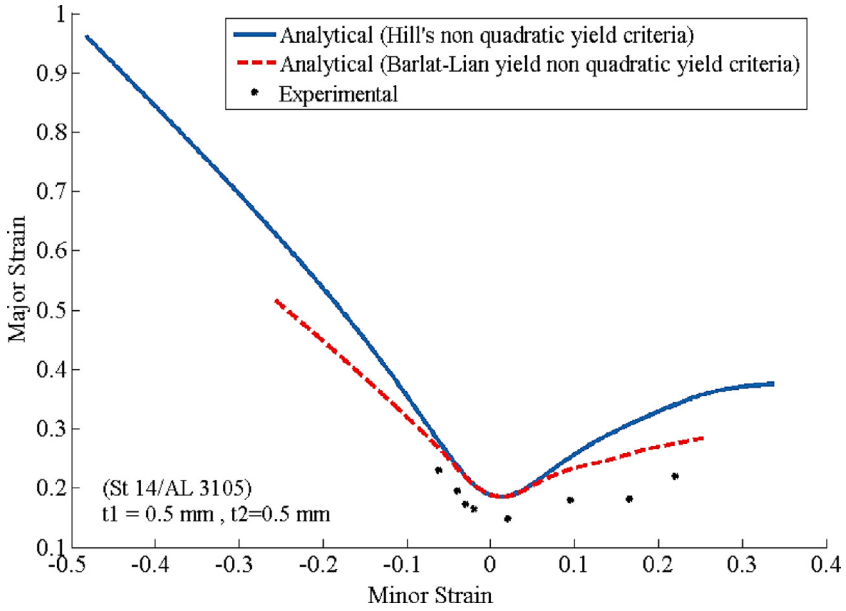

Fig. 7. Comparison of the FLDs obtained from analytical models and experimental results.

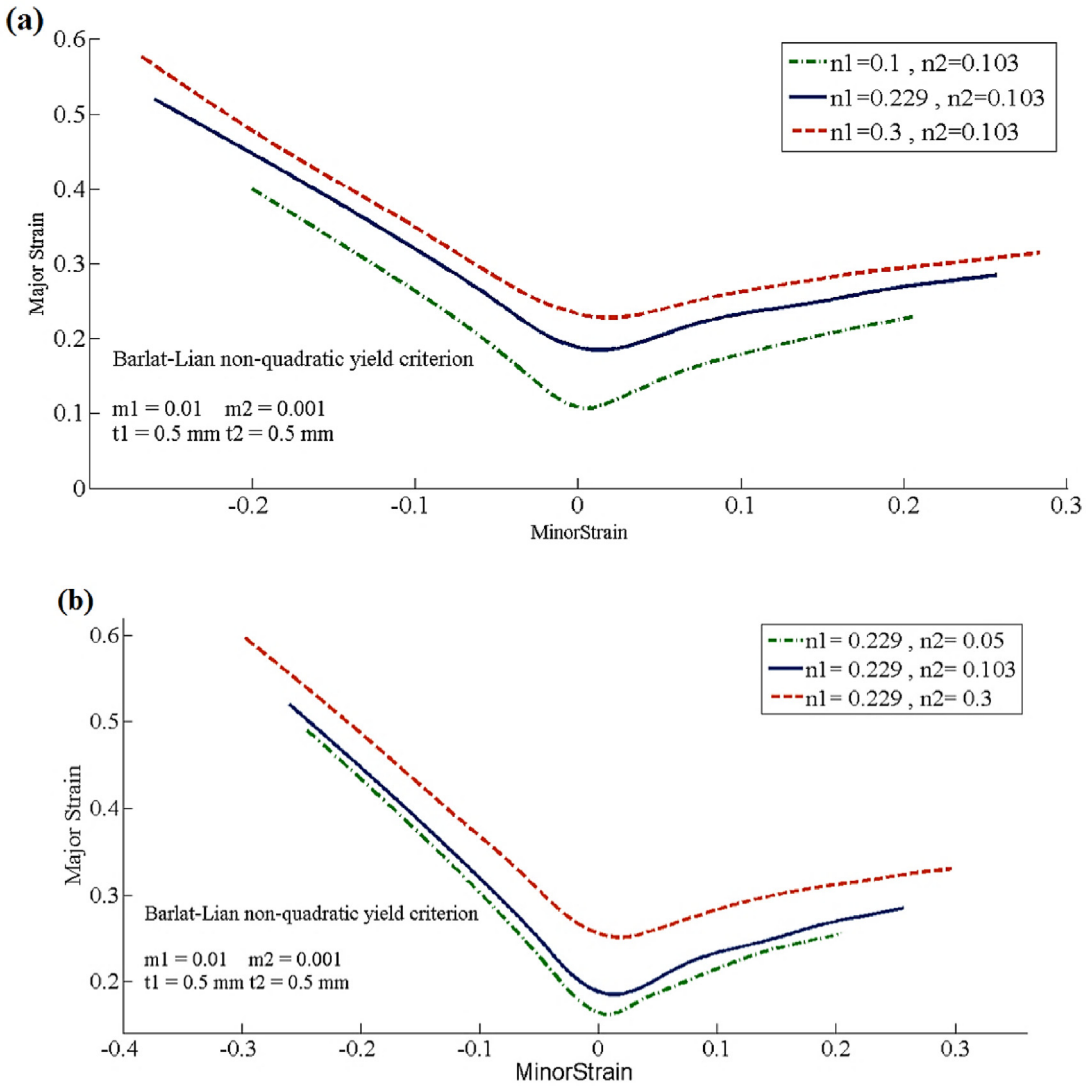

Fig. 8. (a) Effect of the strain hardening exponent of on the FLD of two-layer sheet: (a) n_1 variant, (b) n_2 variant.

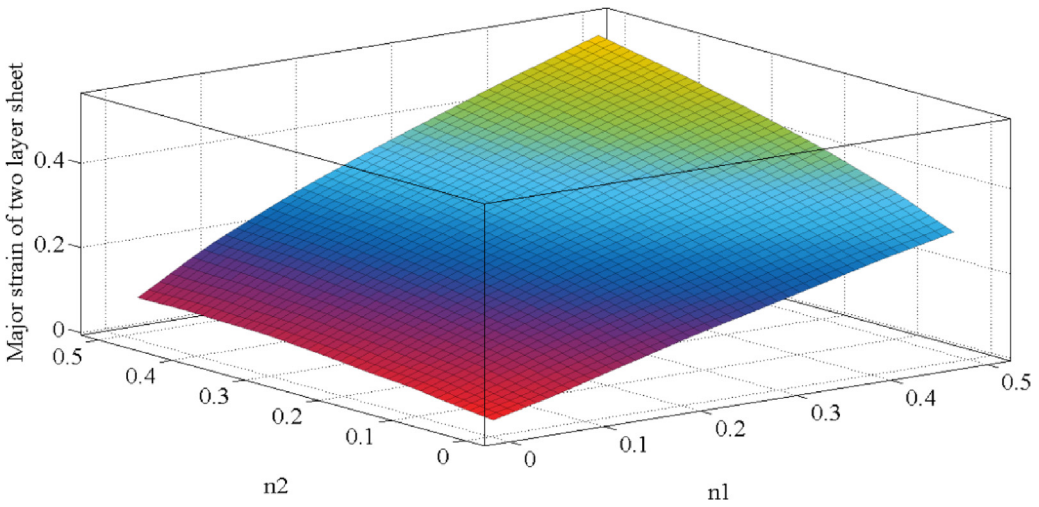

Fig. 9. The simultaneous effects of the strain hardening exponents of layers on FLD_0.

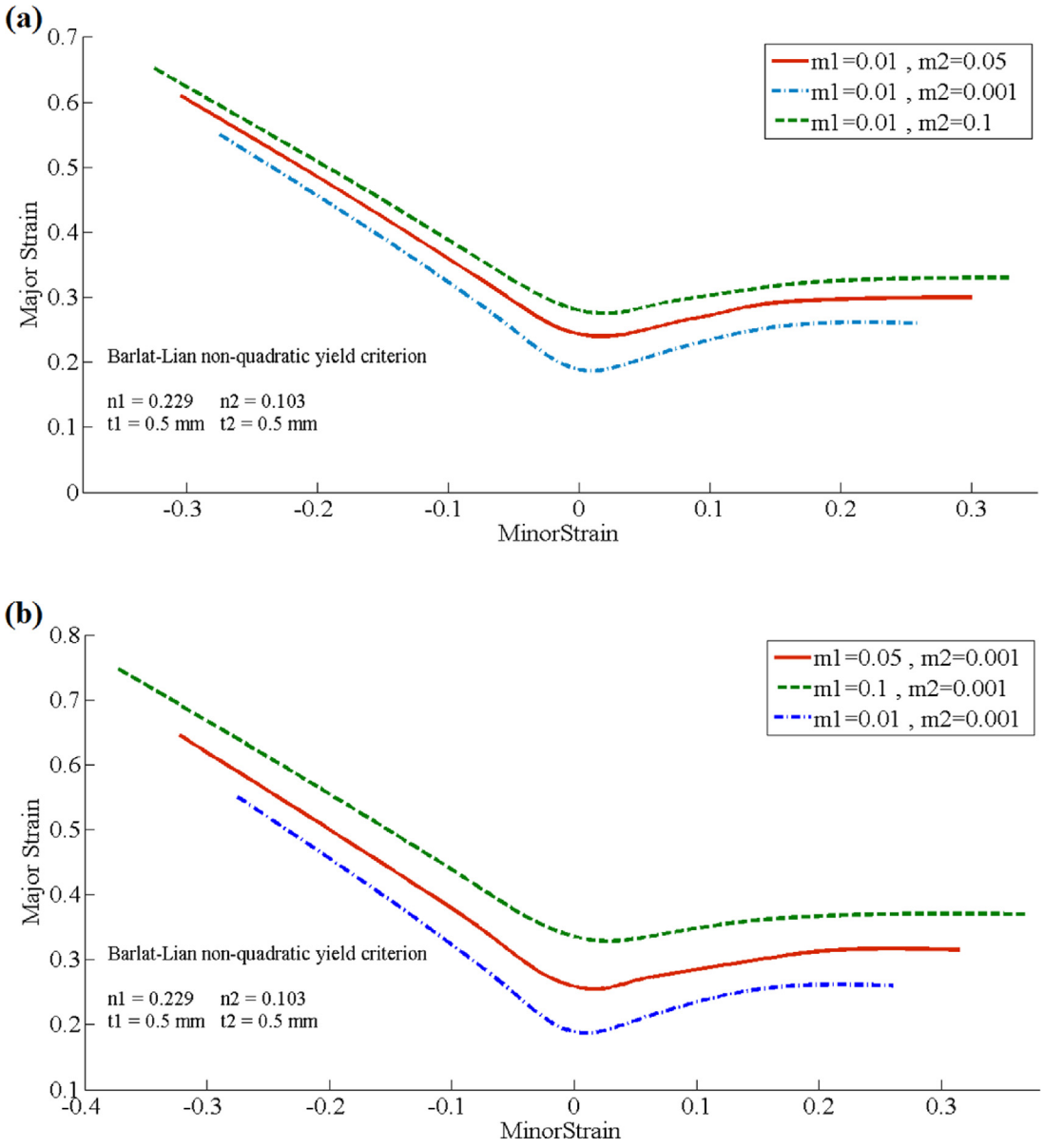

Fig. 10. (a) the effect of strain rate sensitivity on the FLD of two-layer sheet: (a) m_1 variant, (b)m_2 variant.

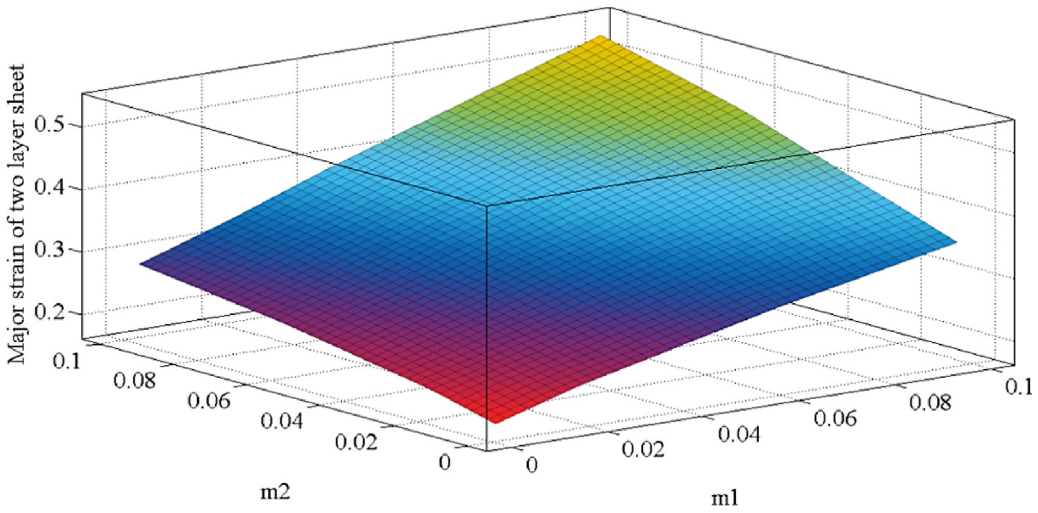

Fig. 11. A simultaneous effect of the strain rate sensitivity exponent of layers on FLD_0.

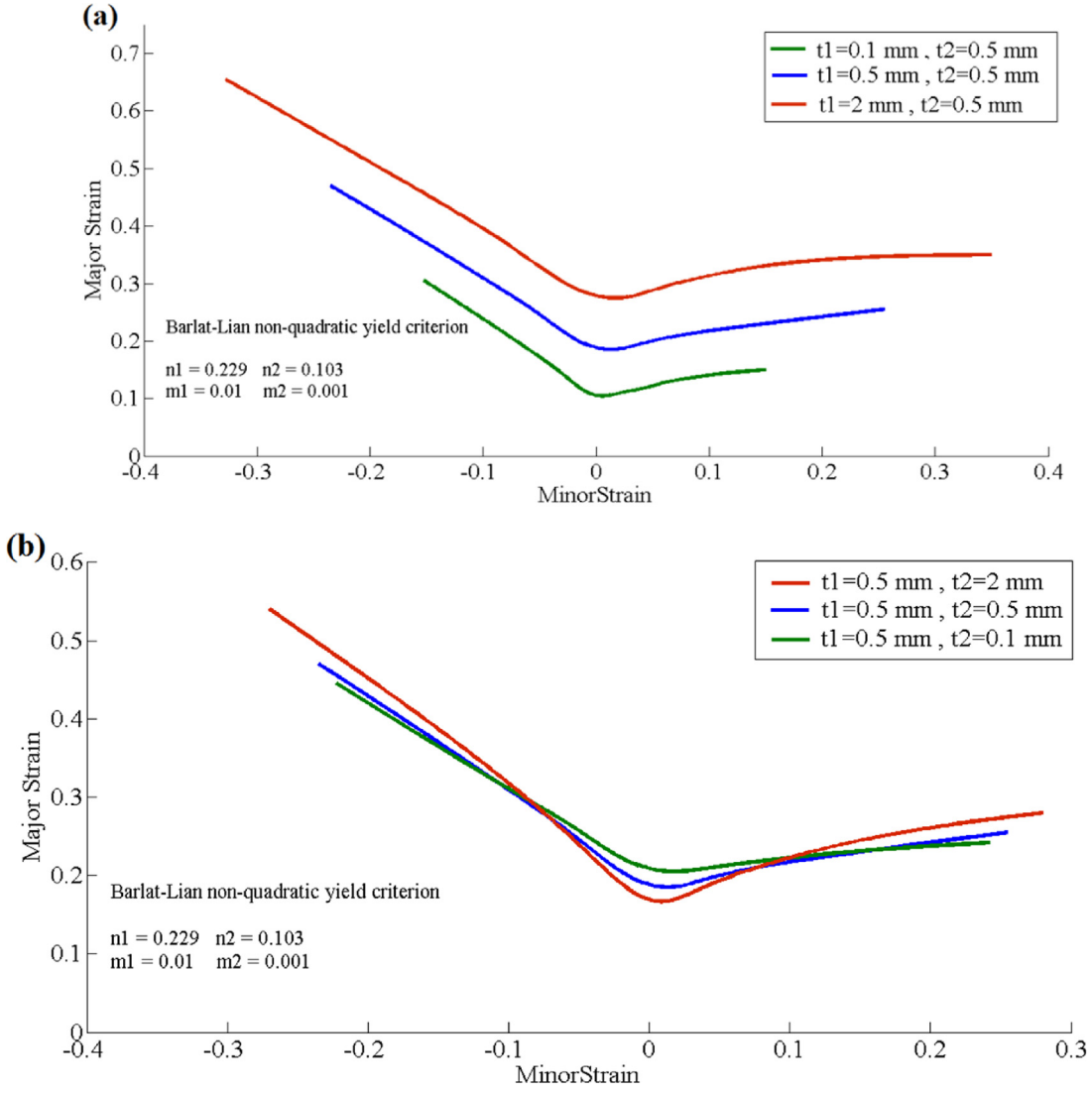

Fig. 12. The effect of thickness of layers on the FLD of two-layer sheet: (a) t_1 variant, (b) t_2 variant.

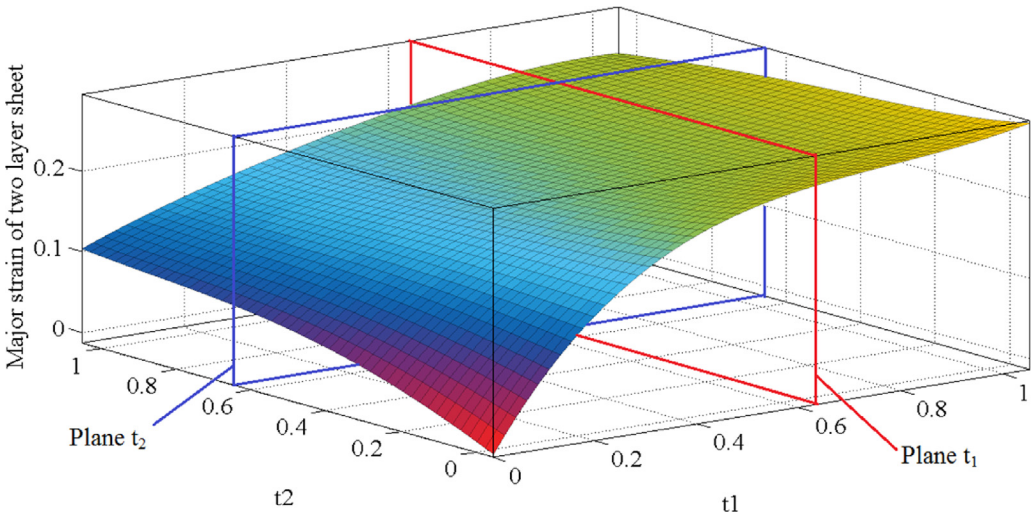

Fig. 13. Effect of the thickness of layers on FLD_0 of two-layer sheet.

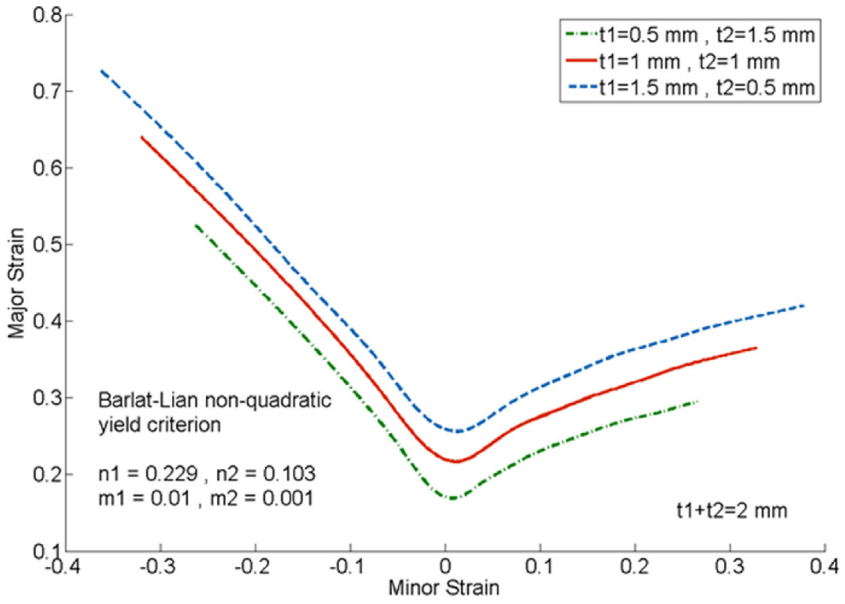

Fig. 14. The effect of the thickness ratio of layers on the FLD of two-layer sheet.

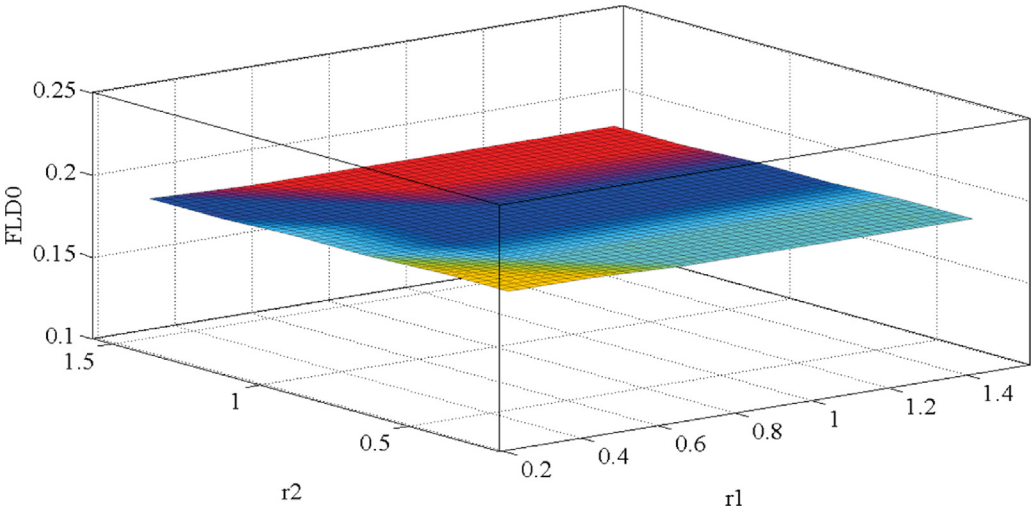

Fig. 15. The effect of simultaneous changes of anisotropy parameters of layers on the FLD_0.

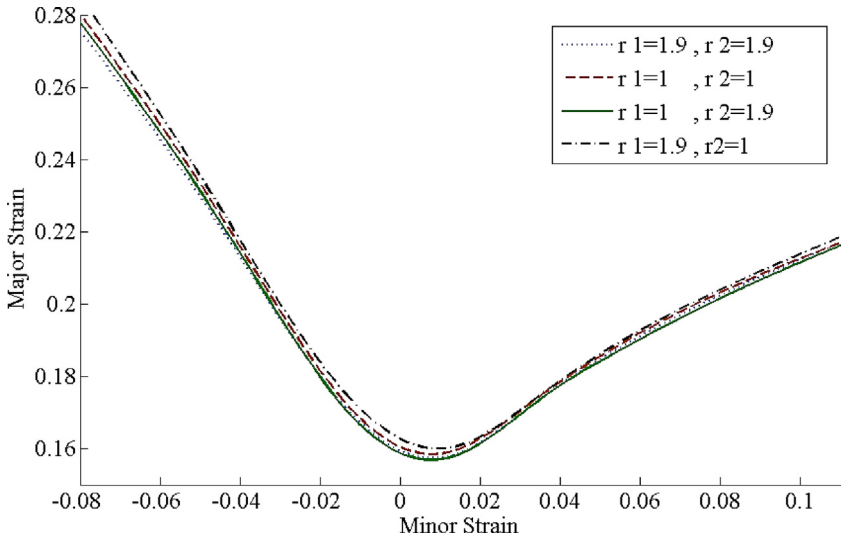

Fig. 16. Effect of anisotropy/isotropy sheet.

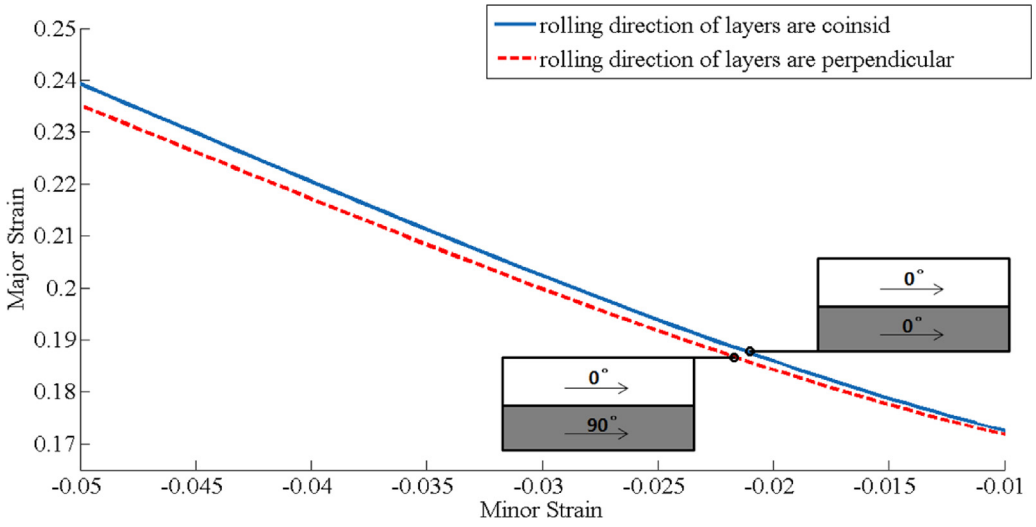

Fig. 17. Effect of anisotropy/isotropy sheet.

hardening exponent of layer 1 (n_1), which is related to the layer with higher formability (means "St-14" layer), changes from 0.005 to 0.3, while the strain hardening exponent of layer 2 (n_2) related to the layer with lower formability (means "AL-3105" layer) keeps constant. Likewise, in the Fig. 8b, the exponent n_2 changes from 0.05 to 0.3 and the exponent n_1 is constant. The results indicate that the formability of two-layer sheet improves with increasing the n value of each layer because of the key role of hardening exponent of sheet material to resist necking phenomenon in the sheet metal forming. Also, it can be found that the effect of strain hardening exponent of layers on FLD curves is more significant in the plane strain condition while the variation of the FLD curves is lesser in the tensile and biaxial tests condition.

To investigate the effect of strain hardening exponent of each layer on the formability of two-layer sheet in the plane strain condition, the minimum point of the curves (indicates $\ddot{\text{FLD}}_0\ddot{}$) in various n_i (i = 1,2) has been captured. Fig. 9 illustrates the effect of strain hardening exponent variation of both layers on the FLD_0 values of two-layer sheet simultaneously. As in can been clearly seen with comparison of graph slopes, the changes in value n_1 is more effective than n_2 value. It proves that change in strength of layer with higher formability influences more on the formability of whole two-layer sheets. In addition, the maximum value of FLD_0 attains when the sheets with higher strain hardening exponent have been selected for both layers of bimetallic sheet.

4.1.2. *Effect of strain rate sensitivity coefficient of layers*

The effects of strain rate sensitivity coefficient (m_i) of layers on the predicted FLD of two-layer sheet have been investigated in Fig. 10. As seen in Fig. 10a, the m_1 value (related to the high formable layer) changes from 0.01 to 0.1, while the m_2 value (related to the less formable layer), remains constant. Also in Fig. 10b, the m_2 value has been changed from 0.001 to 0.1, while the m_1 value is constant. The results of two figures show that the forming limit diagram of bimetallic sheet rises by the use of higher strain rate sensitivity coefficient for each layer because of better strain distribution on sheet with higher m value during plastic deformation. In fact, the higher m value of sheet similarly, the maximum variation of the predicted FLD curves is demonstrated in the plane strain condition than other left and right sides regions.

The effect of simultaneous changes of the strain rate sensitivity coefficients of each layer on the predicted FLD_0 value of two-layer sheet has been presented in Fig. 11. As it can be seen, the changes of FLD_0 value with altering both coefficients m_1 and m_2 show a rel-

atively linear behavior with different slopes while the slope of line for variable m_1 has more influence on the FLD_0 in respect of the variable m_2. So, the strain rate exponent of layer with higher formability (steel layer here) plays key role to design a high formable two-layer sheet but design thickness of layer will be important to obtain an optimum design of bimetallic sheet with lower weight.

4.1.3. Effect of thickness of layers

One of the main factors in design of materials for two-layer sheet is thickness of layers. The effect of variation in thickness of sheet layers on the formability of St/AL two-layer sheet is investigated in Fig. 12a, b. As seen in Fig. 12a, the thickness of layer 1 (t_1 for steel layer) is changed between 0.1 mm, 0.5 mm and 2 mm while the thickness of layer 2 (t_2 for AL layer) remains constant equal to 0.5 mm. It is clearly observed that increase in thickness of steel layer with increasing of total thickness causes improvement in formability of the corresponding two-layer sheet. The fact is because of two-layer sheet with higher thickness of steel layer can resist more against localized necking in low formable aluminum sheet. Fig. 12b shows the FLD curves of two-layer sheet with variant aluminum thickness against constant thickness of steel layer. The FLD curves for variant aluminum thickness demonstrates two different behaviors in the plane strain condition (FLD_0 point) and tensile/biaxial tension (left and right-hand sides). As shown, increasing of aluminum thickness in plane strain condition cannot improve the formability of two-layer sheet with constant steel layer and also it causes decrease in FLD_0 point relatively. But, increasing of aluminum thickness in tensile test (left-hand side of FLD) and stretching test (right-hand side of FLD) enhance the formability of corresponding two-layer sheet. It can be explained that in tensile and stretching tests, increase in the aluminum thickness assists the two-layer sheet to resist more against necking while another failure mechanism occurs in the plane strain condition due to constraint of two-layer sheet straining in width direction.

FLD_0 values of two-layer sheet with simultaneous variation of both t_1 and t_2 are presented in Fig. 13. A non-linear behavior of FLD_0-t_i curve can be seen in this graph as the effect of high formable sheet thickness (steel layer here) is more effective to increase FLD_0 value than variation of low formable sheet's thickness. As seen, when the t_1=0, the monolithic aluminum sheet with thickness "t_2" shows lower FLD than two-layer AL/St sheet with same aluminum thickness and increase in aluminum thickness causes increase in the FLD of aluminum layer separately. Besides, when thet_2 = 0 (thickness of aluminum), which means monolithic steel sheet, the FLD of steel layer is higher than two-layer sheet with the same steel sheet. Because of the two-layer sheet is fractures at the aluminum layer gradually while the steel layer resists yet. Therefore, from the level of FLD_0 surface graph, it can be concluded that the formability of two-layer sheet is between those of elements which compose it. This conclusion can be observed from initial experimental tests on the single and two-layer sheet in the Fig. 6a obviously.

For both cases of the monolithic aluminum sheet (t_1 = 0) and also monolithic steel sheet (t_2=0), the FLD_0 curve shows an upward trend in which the FLD_0 increases with increase in thickness of monolithic sheets as observed by authors formerly. As indicated in Fig. 13, with adding aluminum thickness in specific steel layer thickness (intersection curve in "Plane t_1"), the FLD_0 curve shows a descending graph from specific thickness, while, adding steel layer to monolithic a defined thickness of aluminum sheet (intersection curve in "Plane t_2") demonstrates an ascending trend. This result proves that thickness of steel layer plays a key role whereas the selection of aluminum thickness needs optimization to earn a high formable two-layer sheet. The thickness ratio of layers can give more valuable data to estimate formability of two-layer sheets.

In many industrial applications, we need to design a product with specified weight and total thickness of bimetallic sheet is constant. For this purpose, an investigation on the effect of thickness variation of each layer with constant total thickness of two-layer as $t_t = t_1 + t_2 = 2$ mm is carried out. Fig. 14 illustrates the effect of thickness ratio of layers (the ratio of the thickness of high formable layer to the thickness of low formable layer, $S = t_{St}/t_{AL}$) on FLD curve of two-layer St/AL sheet. It can be found that increasing the thickness ratio from 0.33 to 3 raises the FLD of two-layer sheet as in plane strain condition, the FLD_0 value increases from 0.165 to 0.260. Besides, increase of thickness ratio leads to increase of bimetallic sheet weight. So, the selection of proper thickness based on desirable formability can be one of the research interests to design optimized bimetallic structures.

4.1.4. Effect of anisotropy factor of layers

The normal anisotropy factor (r) of layers is another parameter of sheets during plastic deformation. Similar to the previous studies, the r_i value for each layer was changed in the range of $0.2 \sim 1.6$ while the another one was constant. The results showed a negligible change in the obtained FLD curves of two-layer sheet. As seen in Fig. 15, a nearly horizontal planar surface from the predicted FLD_0 was achieved by simultaneous change of anisotropy factor of layers.

Another study has been examined on the effect of lay-up of sheet layers with considering four cases of isotropic/anisotropic condition for each layer of two-layer sheet. According to Eq. (15), the $r_i = 1$ gives $c = 1$ which indicates the isotropic sheet against assumption of the $r_i = 1.9$ and $c = 1.31$ for anisotropic sheet. The obtained FLD curves of two-layer sheet composed of four states is shown in Fig. 16. As seen in this figure, the anisotropic condition of high formable sheet combined with isotropic condition for low formable sheet can improve formability of two-layer sheets slightly. It can be concluded that lay-up of sheet layers based on combination of isotropic or anisotropic layers in two-layer sheet has inconsiderable influence unlike that other material parameters of layers.

The result of investigation of the influence of lay-up of sheet layers on formability of bimetallic sheet based on rolling direction (called 0° direction) of layers is demonstrated in Fig. 17. As shown in this figure, in the left-hand side of FLD curve, the formability of two-layer sheet increases slightly when the sheet layers is arranged as rolling direction of sheets are aligned (0°-0° lay-up) against perpendicular arrangement of layers (0°-90° lay-up). An explanation for this fact is because of higher strength in rolling direction that is intensified when both layers are arranged in same direction. Unlike, the right-hand side of FLD curve in biaxial stretching condition is remained unchanged. As a result, the selection of 0°-0° arrangement of layers can partly increase formability of two-layer sheet.

5. Conclusions

In this paper, an analytical model based on the M-K theory using Barlat-Lian and Hill's non-quadratic yield function was developed to study the formability of two-layer sheets. Experiments are also carried out on AL3105-St14 two-layer sheet to validate analytical model. Accordingly, the influence of material properties and arrangement of layers on the formability of two-layer sheet was investigated. The results showed that the obtained FLD using Barlat-Lian yield function has better compatibility with experiments in comparison with the results of Hill's yield function for AL3105/St14 two-layer sheet. The obtained results from parametric studies can be drawn as follows:

- The formability of two-layer sheet improves with increasing the values of strain hardening exponents (n_i) and the strain rate sensitivity coefficients (m_i) of its components. The most effect of these factors was observed in the plane strain condition on FLD_0 values.

- The n_i and m_i coefficients of the layer with higher formability showed more significant effect on FLD_0 of two-layer sheet than those of the less formable layer.
- A non-linear behavior was observed with variation of thickness of layers. Generally, the increasing of thickness of layers causes formability enhancement but higher thickness of low formable layer (aluminum) leads to a lower FLD_0 value in the plain strain condition. The thickness of high formable layer (steel) plays a key role. Also, considering a constant thickness for two-layer sheet, increasing the thickness ratio ($t_t S/t_{AL}$) makes the formability of two-layer sheet better. Then, the value of for a two-layer sheet depends on the thickness ratio of layers.
- The rate of change in FLD curve of two-layer sheet due to variation of anisotropy factors of its layers was negligible. However, arrangement of a high formable anisotropic sheet with low formable isotropic sheet can improve formability of two-layer composite sheet slightly. In addition, the arrangement of layers as 0°–0° in aligned rolling direction is recommended to reach better formability of two-layer sheet.
- The proposed model and the obtained results can be helpful greatly to product design by using the applicable two-layer sheets in the manufacturing processes successfully.

Appendix A.

The ratio of the increments of principal strains (ρ) can be derived according to the two yield functions Hill and Barlat-Lian and using "α" (the ratio of principal stresses). The ρ value of each layer (i=1, 2) can be represented for both yield function models as follow:

$$\rho^{a(i)orb(i)} = \frac{d\varepsilon_2^{a(i)orb(i)}}{d\varepsilon_1^{a(i)orb(i)}} = \frac{|1+\alpha^{aorb(i)}|^{M^{(i)}-1} - \left(2r^{(i)}+1\right)|1-\alpha^{aorb(i)}|^{M^{(i)}-1}}{|1+\alpha^{aorb(i)}|^{M^{(i)}-1} + \left(2r^{(i)}+1\right)|1-\alpha^{aorb(i)}|^{M^{(i)}-1}} \tag{A1}$$

$$\rho^{a(i)orb(i)} = \frac{d\varepsilon_2^{a(i)orb(i)}}{d\varepsilon_1^{a(i)orb(i)}} = \frac{u^{(i)}|u^{(i)}\alpha^{(i)}|^{A^{(i)}-1} - \frac{c^{(i)}u^{(i)}}{2-c^{(i)}}|1-u^{(i)}\alpha^{(i)}|^{A^{(i)}-1}}{1+\frac{c^{(i)}}{2-c^{(i)}}|1-u^{(i)}\alpha^{(i)}|^{A^{(i)}-1}} \tag{A2}$$

Using the defined ρ values and incompressibility condition, the thickness strain of each material of two-layer sheet is computed as below:

$$d\varepsilon_3^{a(i)orb(i)} = -\left(1+\rho^{a(i)orb(i)}\right) d\varepsilon_1^{a(i)orb(i)} \tag{A3}$$

In addition, the ratio of principal stress (σ_1) to effective stress ($\bar{\sigma}$) which was defined as variable "φ" is given for both yield functions Hill and Barlat-Lian respectively:

$$\varphi^{a(i)orb(i)} = \frac{\sigma_1}{\bar{\sigma}} = \left[\frac{2\left(r^{(i)}+1\right)}{|1+\alpha^{a(i)orb(i)}|^{M^{(i)}} + \left(2r^{(i)}+1\right)|1-\alpha^{aorb(i)}|^{M^{(i)}}}\right]^{\frac{-1}{M^{(i)}}} \tag{A4}$$

$$\varphi^{a(i)orb(i)} = \frac{\sigma_1}{\bar{\sigma}} = \frac{2}{2-c^{(i)}}\left(1+|u^{(i)}\alpha^{(i)}|^{A^{(i)}} + \frac{c^{(i)}}{2-c^{(i)}}|1-u^{(i)}\alpha^{(i)}|^{A^{(i)}}\right)^{-1} \tag{A5}$$

The "β" value, which is specified as the ratio of effective strain ($d\bar{\varepsilon}$) to principal strain increments ($d\varepsilon_1$), can be expressed for both Hill and Barlat-Lian yield functions respectively as:

$$\beta^{a(i)orb(i)} = \frac{d\bar{\varepsilon}}{d\varepsilon_1} = \varphi^{a(i)orb(i)}\left(1+\alpha^{a(i)orb(i)}\rho^{a(i)orb(i)}\right) \tag{A6}$$

$$\beta^{a(i)orb(i)} = \frac{d\bar{\varepsilon}}{d\varepsilon_1} = \frac{\frac{2}{2-c^{(i)}}\left(\varphi^{a(i)orb(i)}\right)^{A^{(i)}-1}}{1+\frac{c^{(i)}}{2-c^{(i)}}|1-u^{(i)}\alpha^{(i)}|^{A^{(i)}-1}} \tag{A7}$$

References

[1] Maleki H, Bagherzadeh S, Mollaei-Dariani B, Abrinia K. Analysis of bonding behavior and critical reduction of two-Layer strips in clad cold rolling process. J Mater Eng Perform 2013;22:917–25, http://dx.doi.org/10.1007/s11665-012-0342-9.

[2] Takuda H, Mori K, Fujimoto H, Hatta N. Fracture prediction in stretch forming using finite element simulation combined with ductile fracture criterion, 67; 1997.

[3] Tajyar A, Masoumi A. Investigation of mechanical properties of bimetallic square tubes produced by shape rolling of Al/Cu circular pipes. J Mech Sci Technol 2016;30:4299–306, http://dx.doi.org/10.1007/s12206-016-0844-8.

[4] Keeler SP. Circular grid system-A valuable aid for evaluating sheet metal formability. SAE Tech. Pap., SAE International 1968, http://dx.doi.org/10.4271/680092.

[5] Goodwin GM. Application of strain analysis to sheet metal forming problems in the press shop. SAE Tech. Pap., SAE International 1968, http://dx.doi.org/10.4271/680093.

[6] Semiatin SL, Piehler HR. Formability of sandwich sheet materials in plane strain compression and rolling. Metall Trans A 1979;10:97–107, http://dx.doi.org/10.1007/BF02686412.

[7] Semiatin SL, Piehler HR. Deformation of sandwich sheet materials in uniaxial tension. Metall Trans A 1979;10:85–96, http://dx.doi.org/10.1007/BF02686411.

[8] Mori T, Kurimoto S. Press-formability of stainless steel and aluminum clad sheet. J Mater Process Technol 1996;56:242–53, http://dx.doi.org/10.1016/0924-0136(95)01838-7.

[9] Yoshida F, Hino R. Forming limit of stainless steel-clad aluminium sheets under plane stress condition. J Mater Process Technol 1997;63:66–71, http://dx.doi.org/10.1016/S0924-0136(96)02601-5.

[10] Kim KJ, Kim D, Choi SH, Chung K, Shin KS, Barlat F, et al. Formability of AA5182/polypropylene/AA5182 sandwich sheets. J Mater Process Technol 2003;139:1–7, http://dx.doi.org/10.1016/S0924-0136(03)00173-0.

[11] Jalali Aghchai A, Shakeri M, Mollaei Dariani B. Influences of material properties of components on formability of two-layer metallic sheets. Int J Adv Manuf Technol 2013;66:809–23, http://dx.doi.org/10.1007/s00170-012-4368-9.

[12] Aghchai AJ, Shakeri M, Mollaei-Dariani B. Theoretical and experimental formability study of two-layer metallic sheet (Al1100/St12). Proc Inst Mech Eng Part B J Eng Manuf 2008;222:1131–8, http://dx.doi.org/10.1243/09544054JEM1140.

[13] Bagherzadeh S, Mollaei-dariani B, Malekzadeh K. Journal of Materials Processing Technology Theoretical study on hydro-mechanical deep drawing process of bimetallic sheets and experimental observations. J Mater Process Tech 2012;212:1840–9, http://dx.doi.org/10.1016/j.jmatprotec.2012.04.002.

[14] Bagherzadeh S, Mirnia MJ, Dariani BM. Numerical and experimental investigations of hydro-mechanical deep drawing process of laminated aluminum/steel sheets. J Manuf Process 2015;18:131–40, http://dx.doi.org/10.1016/j.jmapro.2015.03.004.

[15] Liu J, Liu W, Xue W. Forming limit diagram prediction of AA5052/polyethylene/AA5052 sandwich sheets. Mater Des 2013;46:112–20, http://dx.doi.org/10.1016/j.matdes.2012.09.057.

[16] Parsa MH, Ettehad M, Al Ahkami SN. FLD determination of AL 3105/Polypropylene/AL 3105 sandwich sheet using numerical calculation and experimental investigations. Int J Mater Form 2009;2:407, http://dx.doi.org/10.1007/s12289-009-0502-0.

[17] Parsa MH, Ettehad M, Matin PH, Al Ahkami SN. Experimental and numerical determination of limiting drawing ratio of al3105-Polypropylene-Al3105 sandwich sheets. J Eng Mater Technol 2010;132:31004, http://dx.doi.org/10.1115/1.4001264.

[18] Dehghani M. Analytical and experimental analysis of the formability of copper-stainless-steel 304L clad metal sheets in deep drawing; 2015, http://dx.doi.org/10.1007/s00170-015-7359-9.

[19] Karajibani E, Hashemi R, Sedighi M. Forming limit diagram of copper two-layer sheets: numerical simulations and experimental verifications. Int J Adv Manuf Technol 2016:1–10, http://dx.doi.org/10.1007/s00170-016-9585-1.

[20] Hashemi R, Karajibani E. Forming limit diagram of Al-Cu two-layer metallic sheets considering the Marciniak and Kuczynski theory; 2016, http://dx.doi.org/10.1177/0954405416654419.

[21] Marciniak Z, Kuczyński K. Limit strains in the processes of stretch-forming sheet metal. Int J Mech Sci 1967;9:609–20, http://dx.doi.org/10.1016/0020-7403(67)90066-5.

[22] Gronostajski JZ, Zimniak Z. Theoretical simulation of sheet behaviour in forming processes. J Mater Process Technol 1992;31:57–63, http://dx.doi.org/10.1016/0924-0136(92)90006-E.

[23] Assempour A, Nurcheshmeh M. The Influence of Material Properties on the Shape and Level of the Forming Limit Diagram. SAE Tech. Pap., SAE International 2003, http://dx.doi.org/10.4271/2003-01-1149.

[24] Swift HW. Plastic instability under plane stress. J Mech Phys Solids 1952;1:1–18, http://dx.doi.org/10.1016/0022-5096(52)90002-1.

[25] Barlat F, Lian K. Plastic behavior and stretchability of sheet metals Part I: A yield function for orthotropic sheets under plane stress conditions. Int J Plast 1989;5:51–66, http://dx.doi.org/10.1016/0749-6419(89)90019-3.

[26] Hill R. Theoretical plasticity of textured aggregates. Math Proc Cambridge Philos Soc 1979;85:179–91, http://dx.doi.org/10.1017/S0305004100055596.

[27] Dariani BM, Azodi HD. Finding the optimum Hill index in the determination of the forming limit diagram. Proc Inst Mech Eng Part B J Eng Manuf 2003;217:1677–83, http://dx.doi.org/10.1243/095440503772680604.

[28] Ghosh AK, Hecker SS. Stretching limits in sheet metals: in-plane versus out-of-plane deformation. Metall Trans 1974;5:2161–4, http://dx.doi.org/10.1007/BF02643929.

[29] Li X, Song N, Guo G, Sun Z. Prediction of forming limit curve (FLC) for Al-Li alloy 2198-T3 sheet using different yield functions. Chinese J Aeronaut 2013;26:1317–23, http://dx.doi.org/10.1016/j.cja.2013.04.011.